Critical behavior of CoO and NiO from specific heat, thermal conductivity, and thermal diffusivity measurements

M. Massot, A. Oleaga, and A. Salazar*
Departamento de Física Aplicada I, Escuela Técnica Superior de Ingeniería, Universidad del País Vasco, Alameda Urquijo s/n, 48013 Bilbao, Spain

D. Prabhakaran
Clarendon Laboratory, Department of Physics, University of Oxford, Oxford OX1 3PU, United Kingdom

M. Martin
Institut für Physikalische Chemie, RWTH Aachen University, Landoltweg 2, 52056 Aachen, Germany

P. Berthet and G. Dhalenne
Université Paris Sud and CNRS, UMR8182, ICMMO/LPCES, Bâtiment 410, F-91405 Orsay cedex, France
(Received 29 October 2007; revised manuscript received 11 February 2008; published 23 April 2008)

An ac photopyroelectric calorimeter has been used to simultaneously measure the specific heat (c_p), thermal conductivity (K), and thermal diffusivity (D) around the antiferromagnetic to paramagnetic phase transition in CoO and NiO single crystals. Up to now, no agreement on the critical behavior of both oxides has been obtained. The results for seven samples grown in different laboratories have been compared. We have found that, irrespective of the origin of the samples, the critical exponent and amplitude ratio of c_p, D, and K in NiO agree with the predictions of the three-dimensional Heisenberg model for isotropic antiferromagnets, which contradicts previous results. On the other hand, the sharpness of the peak of specific heat and of the dip of thermal diffusivity, together with the value of the critical exponent α in CoO, highly increase as crystal quality improves. For the best sample, a value $\alpha=0.81$ has been obtained, which is not only higher than previously reported results, but far away from any universality class.

DOI: 10.1103/PhysRevB.77.134438 PACS number(s): 64.60.Ht, 65.40.−b, 75.40.−s, 75.50.Ee

I. INTRODUCTION

The four transition-metal magnetic monoxides (MnO, FeO, CoO, and NiO), with the NaCl structure (space group $Fm3m$) in their high temperature state, are type-II antiferromagnets: the magnetic spins ferromagnetically align within the (111) plane, while these planes are antiferromagnetically stacked in the direction normal to the (111) plane. At their respective Néel temperature (T_N), they undergo a paramagnetic-antiferromagnetic phase transition coupled to a symmetry breaking: a small rhombohedral distortion in MnO, FeO, and NiO, and a tetragonal distortion in CoO.[1] A renormalization-group analysis suggested that the magnetic phase transition in the four transition-metal monoxides should have a first order nature.[2–4] Experimentally, the transition in MnO and FeO has been established to be first order.[5–10] On the other hand, CoO has been traditionally considered to be second order according to different types of experimental measurements.[11–17] However, when analyzing the critical behavior, no agreement has been obtained: some of the results are close to those predicted by the three-dimensional (3D) Ising model,[11,12,17] but a 3D-Heisenberg behavior has also been reported.[15,16] Moreover, a recent crystallographic study suggests that the transition should be discontinuous since the magnetic ordering is coupled to a cubic to monoclinic symmetry breaking, in addition to the already known tetragonal distortion.[18] Therefore, the critical behavior and even the nature of the magnetic transition in CoO are still controversial. In its turn, the transition in NiO is clearly second order.[19–21] However, no agreement on the universality class to which it belongs has been obtained yet: the obtained values of the critical exponent β from measurements of spontaneous magnetization[19] and magnetic birefringence[21] are in between the predictions of the 3D-Heisenberg and 3D-Ising models, although closer to the last one.

In this work, we use a photopyroelectric calorimeter to simultaneously measure the specific heat (c_p), thermal conductivity (K), and thermal diffusivity (D) around the magnetic transition of CoO and NiO single crystals. We present accurate measurements of K and D through the magnetic phase transition in these single oxides. Actually, few high-resolution data of the thermal conductivity and diffusivity for solid samples are available in literature.[22–27] This is due to the conflict between the need of producing thermal gradients for thermal transport measurements and the need of keeping them as small as possible for not destroying the critical information. In this way, the ac photopyroelectric calorimetry[28,29] is especially tailored for the measurement of the thermal transport properties around phase transitions, since small temperature gradients in the sample produce a good signal-to-noise ratio, which allows thermal properties be measured with high accuracy. Our aim is to study the critical behavior of the thermophysical properties of NiO and CoO in order to elucidate the universality class to which each monoxide belongs.

II. EXPERIMENTAL SETUP AND RESULTS

Simultaneous measurements of K, D, and c_p were performed by a high-resolution ac photopyroelectric calorimeter

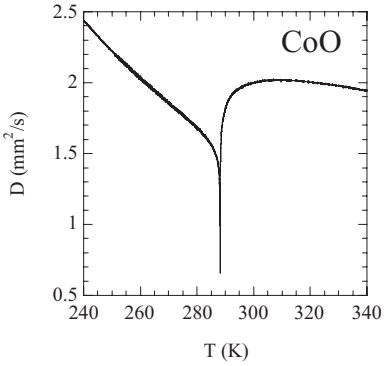

FIG. 1. Temperature dependence of D for CoO over a wide temperature range.

used in the standard back-detection configuration.[27,28] An acousto-optically modulated He-Ne laser beam of 5 mW illuminates the front surface of the sample under study. Its rear surface is in thermal contact with a 350 μm thick $LiTaO_3$ pyroelectric detector with Ni-Cr electrodes on both surfaces, by using an extremely thin layer of a highly heat-conductive silicone grease (Dow Corning, 340 Heat Sink Compound). The photopyroelectric signal is processed by a lock-in amplifier operating in the current mode. Both sample and detector are placed inside a nitrogen bath cryostat (77–310 K) or an oven (300–600 K). Measurements are performed at rates that vary from 100 mK/min for measurements on a wide temperature range up to 10 mK/min for high-resolution runs close to the phase transitions.

For opaque and thermally thick samples (i.e., the thickness of the sample is higher than the thermal diffusion length $\mu=\sqrt{D/\pi f}$, where f is the modulation frequency of the laser beam) the natural logarithm ($\ln V$) of the amplitude of the normalized photopyroelectric signal (which is obtained by dividing the measured signal by the signal provided by the bare detector) and its phase (Ψ) have a linear dependence on $\sqrt{f}$, with the same slope. From their slope m and from the vertical separation between the two straight lines d, the thermal diffusivity and the thermal effusivity ($e=\sqrt{\rho c_p K}=K/\sqrt{D}$) of the sample can be obtained[29] as follows:

$$D=\frac{\pi\ell^2}{m^2}, \tag{1}$$

$$e=e_p\left(\frac{2}{\exp(d)}-1\right), \tag{2}$$

where ρ is the density, ℓ is the sample thickness, and e_p is the thermal effusivity of the pyroelectric detector.

Once thermal diffusivity and effusivity have been measured at a certain reference temperature (T_{ref}, D_{ref}, and e_{ref}), the temperature is changed while recording the amplitude and phase of the pyroelectric signal at a fixed frequency. The temperature dependence of D and e are given by[29,30]

$$D(T)=\left(\frac{1}{\sqrt{D_{ref}}}-\frac{\Delta(T)}{\ell\sqrt{\pi f}}\right)^{-2}, \tag{3}$$

$$e(T)=e_p(T)\left(\frac{1+\dfrac{e_{ref}}{e_p(T_{ref})}}{\exp[\Delta''(T)]}-1\right), \tag{4}$$

where $\Delta(T)=\Psi(T)-\Psi(T_{ref})$, $\Delta'(T)=\ln V(T)-\ln V(T_{ref})$, and $\Delta''(T)=\Delta'(T)-\Delta(T)$. Finally, the temperature dependence of specific heat and thermal conductivity are calculated from the following relations:

$$c_p(T)=\frac{e(T)}{\rho\sqrt{D(T)}}, \tag{5}$$

$$K(T)=e(T)\sqrt{D(T)}. \tag{6}$$

We have measured several single crystal plates of each oxide coming from different growers: four CoO samples, labeled 1–4, and three NiO samples. All thicknesses are between 500 and 600 μm. A modulation frequency of 8.0 Hz, which is high enough to assure that the sample is thermally thick but low enough to guarantee a good signal-to-noise ratio, has been used. It has been tested that measurements performed at other close frequencies give the same values of c_p, K, and D.

In Fig. 1, the temperature dependence of D for CoO over a wide temperature range around the magnetic transition is shown. In this scale, there is no difference among the four samples we have measured. As can be seen, the transition temperature is marked by a very sharp dip in thermal diffusivity. In Fig. 2, the temperature dependence of c_p, K, and D close to T_N is shown to better appreciate the difference in sharpness of the peak in specific heat and the dip in thermal

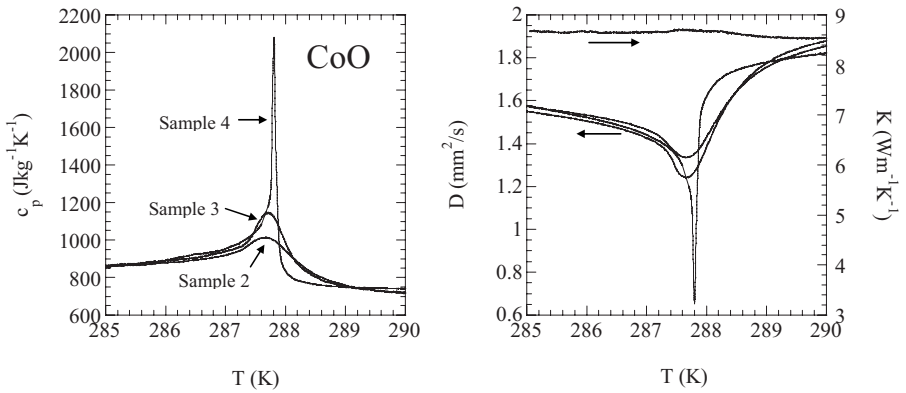

FIG. 2. Temperature dependence of c_p, K, and D around T_N for three different CoO crystals (samples 2, 3, and 4).

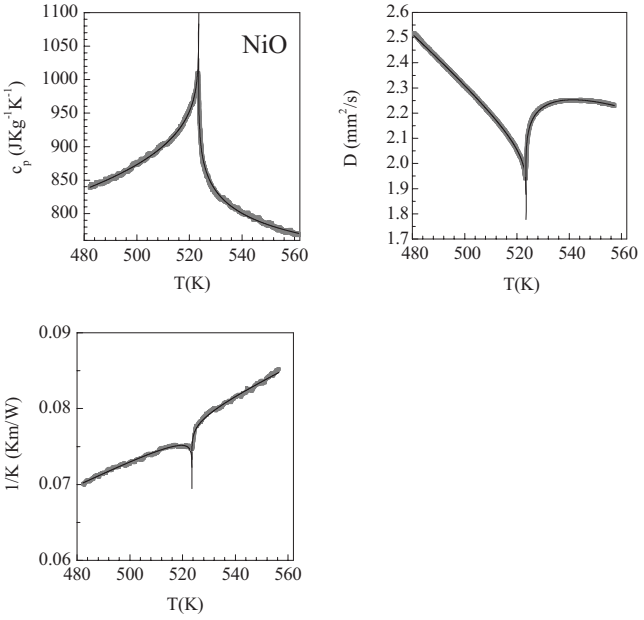

FIG. 3. Temperature dependence of c_p, D, and $1/K$ around T_N for NiO. Dots are the experimental data and the lines correspond to the best fits.

diffusivity, according to the sample quality. Actually, for samples 1 and 2, we obtained the same shallow peak or dip (only the results for sample 2 are shown). It is worth noting that this blunt specific heat is similar to all previously reported in literature.[11,15,17] Sample 3 exhibits a sharper feature, whereas sample 4 shows a high sharpness, which indicates the higher quality of this crystal (high purity, better stoichiometry, fewer defects, etc.). However, even for this sample, no thermal hysteresis has been found. Finally, note that K does not present any anomaly, which is in agreement with previous results.[15]

In Fig. 3, the temperature dependence of c_p, D, and $1/K$ around the magnetic transition temperature for NiO is shown by dots. As can be seen, the D values are very accurate since they are directly obtained from the phase of the photopyroelectric signal [see Eq. (3)], while the c_p and $1/K$ values are affected by a higher uncertainty since they are obtained by combining both amplitude and phase [see Eqs. (5) and (6)]. The peak in c_p (dip in D) shows the typical λ shape (inverted λ shape) with no hysteresis characteristic of a second order phase transition. On the other hand, $1/K$ shows a shallow dip at T_N, similar to those found for other magnetic materials such as FeF_2, $RbMnF_3$, and $KMnF_3$.[24,26,31] Note that the scale for $1/K$ has been chosen so as to show that its singularity is much smaller than those obtained for c_p and D. It is also worth noting that no noticeable differences have been found for the three crystals, coming from different growers.

III. FITTING PROCEDURE AND DISCUSSION

In this section, we concentrate on the study of the critical behavior of the magnetic transition of both CoO and NiO. The critical behavior of the specific heat in second order phase transitions is described by a function of the form

$$c_p = B + Ct + A^{\pm}|t|^{-\alpha}(1 + E^{\pm}|t|^{0.5}), \tag{7}$$

where $t=(T-T_N)/T_N$ is the reduced temperature, and α, $A^{\pm}$, B, C, and $E^{\pm}$ are adjustable parameters. Superscripts + and − stand for $T>T_N$ and $T<T_N$, respectively. The linear term represents the background contribution to the specific heat, while the last term is the anomalous contribution to the specific heat. The factor within parentheses is the correction to scaling that represents a singular contribution to the leading power as known from experiments and theory.[32,33]

For thermal diffusivity and thermal conductivity, we assume, similar to the specific heat, that they are given by a sum of a regular term plus a singular one, with a correction to scale term,[26] as follows:

$$D = V + Wt + U^{\pm}|t|^{-b}(1 + F^{\pm}|t|^{0.5}), \tag{8}$$

$$1/K = 1/K_{nonmag} + 1/K_{mag} = L + Mt + N^{\pm}|t|^{-g}(1 + H^{\pm}|t|^{0.5}). \tag{9}$$

Subindex "nonmag" refers to phonon-phonon scattering, umklapp, scattering with impurities, etc., while "mag" refers to the spin-phonon scattering mechanisms. The magnetic resistive term originates from the spin-lattice interaction and close to T_N from an additional term that accounts for phonon scattering by critical fluctuations of the order parameter. The reason for fitting the $1/K$ data instead of the K ones relies on the fact that all of the thermal resistances associated with the various heat conduction mechanisms in the sample are in series. In this way, the singular term in Eq. (9) can be related to the magnetic contribution to the heat conduction processes.

The experimental data were simultaneously fitted for $T>T_N$ and $T<T_N$ with a nonlinear least square routine by using a Levenberg–Marquardt method. First of all, we selected a fitting range close to the peak (dip) while avoiding the rounding, and kept fixed the value of T_N. We obtained a first fitting without the correction to scaling term and obtained a set of adjusted parameters. Afterwards, we tried to increase the number of points included in the fitting, first fixing t_{min} and increasing t_{max}, and then fixing t_{max} and decreasing t_{min}. The next step was to introduce the correction to the scaling term to try to improve the fitting. As a final check, we let T_N be a free parameter in order to confirm the fitting. In the whole process, we focused our attention on the root mean square values as well as on the deviation plots, which are the plots of the difference between the fitted values and the measured ones as a function of the reduced temperature.

A. NiO

The continuous lines in Fig. 3 represent the fittings of the experimental data to Eqs. (7)–(9). In Fig. 4, the deviation plots show the range of the reduced temperatures used in the fittings as well as their quality. The values of the fitting parameters are given in Table I. It is seen that the values of the critical exponent and the amplitude ratio of the specific heat are in good agreement with the predictions of the 3D-Heisenberg model for isotropic magnets [$\alpha=-0.115$ and

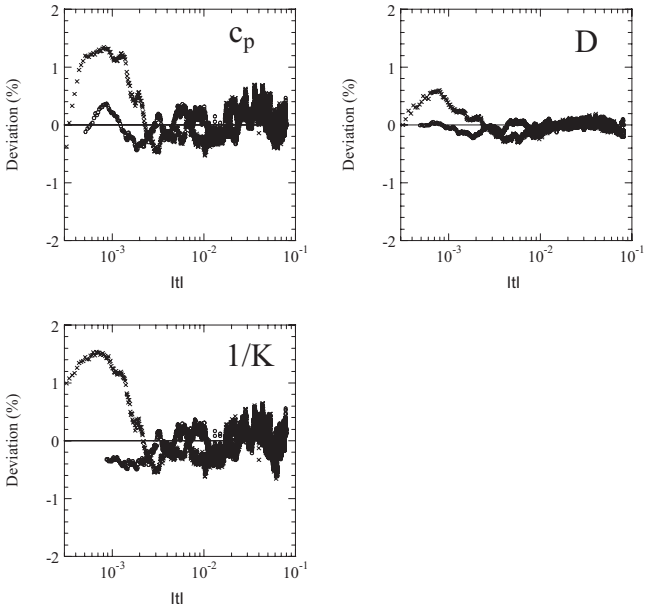

FIG. 4. Deviation plots corresponding to the fits of Fig. 3 for NiO. Open circles are for $T<T_N$ and crosses for $T>T_N$.

$A^+/A^-=1.58$ (Refs. 34 and 35)] in a wide temperature range ($|t|=4\times10^{-4}-8\times10^{-2}$ for $T>T_N$ and $|t|=7\times10^{-4}-8\times10^{-2}$ for $T<T_N$).[36] On the other hand, the critical exponent and the amplitude ratio of the thermal diffusivity are very similar to those found for specific heat, a result that was already found in isotropic antiferromagnets.[26,31] They agree with the predictions by Pawlak[37] about the critical thermal diffusivity of isotropic magnets, which follow the phenomenological hydrodynamical approach to critical dynamics: $b=\alpha$ and $U^+/U^-=A^+/A^-$. From these results, we can conclude that the magnetic transition in NiO is second order and agrees with the 3D-Heisenberg universality.

The singular term of $1/K$ has a positive amplitude ($N^+,N^->0$) and a negative exponent ($g<0$), which indicates that the thermal conductivity does not diverge at T_N. Moreover, the values of the critical exponent and the amplitude ratio ($g=-0.11$ and $N^+/N^-=1.3$) are very similar to those found for other isotropic antiferromagnets.[26,31] They are close to those expected for the 3D-Heisenberg model for specific heat, although their meaning is not well understood yet. In fact, according to the existing theories on the critical behavior of thermal conductivity, no divergence should be expected for K.[38–40] However, these theories are largely incomplete and recent high-resolution thermal conductivity measurements show small but not negligible peaks close to the transition temperature for some materials (FeF_2, $RbMnF_3$, and $KMnF_3$),[24,26,31] while for other materials (EuO, MnO, CoO, and Cr_2O_3) no anomaly was found.[15,22,23] Anyway, it is worth noting that whenever isotropic materials show a singularity in thermal conductivity, the critical parameters for $1/K$ are close to those predicted for c_p, as is the case of $RbMnF_3$, $KMnF_3$, and NiO in this work.[26,31]

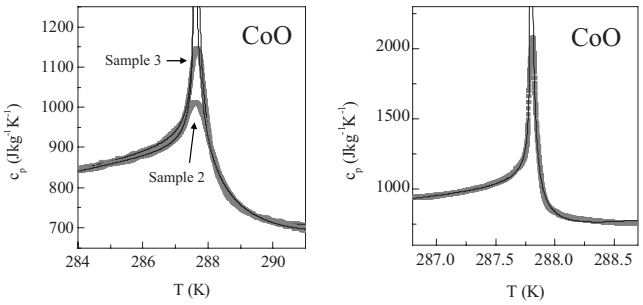

FIG. 5. Temperature dependence of c_p in close vicinity of T_N for the same three CoO crystals as in Fig. 2. On the left, the results for samples 2 and 3 are shown, whereas the results for sample 4 are shown on the right. Dots are the experimental data and the lines correspond to the best fits

B. CoO

In Fig. 5, we show the specific heat data for the three CoO crystals of Fig. 2, in close vicinity of T_N. On the left, the results in c_p for samples 2 and 3, which show a broader transition, are presented, while on the right, the result for

TABLE I. Values of the adjustable fitting parameters for specific heat, thermal diffusivity, and the inverse of thermal conductivity for NiO. In bold are the universal parameters. R is the deviation coefficient.

	α	A^+/A^-	T_N (K)	B (J kg^{-1} K^{-1})	E (J kg^{-1} K^{-1})	A^- (J kg^{-1} K^{-1})	D^{-1}	D^{+1}	R
c_p (J kg^{-1} K^{-1})	**−0.118**	**1.63**	523.62	1170	−220	−360	1.1	−0.40	0.9985
	±0.006	**±0.006**	±0.05	±12	±43	±12	±0.1	±0.07	
	b	U^+/U^-	T_N (K)	V (mm^2/s)	W (mm^2/s)	U^- (mm^2/s)	F^-	F^+	R
D (mm^2/s)	**−0.125**	**1.60**	523.45	1.76	−4.29	0.485	0.44	1.41	0.9995
	±0.006	**±0.04**	±0.05	±0.01	±0.03	±0.008	±0.03	±0.05	
	g	N^+/N^-	T_N (K)	L (Km/W)	M (Km/W)	N^- (Km/W)	H^-	H^+	R
$1/K$ (Km/W)	**−0.11**	**1.3**	523.5	0.069	0.093	0.012	−0.20	−0.6	0.9980
	±0.02	**±0.02**	±0.05	±0.001	±0.002	±0.001	±0.06	±0.02	

TABLE II. Values of the critical exponent for the specific heat (α) and the range of reduced temperature (t) used in the fittings for the three CoO samples.

	α	$t_{max}-t_{min}$ ($T<T_N$)	$t_{max}-t_{min}$ ($T>T_N$)	R
Sample 2 (poor quality)	**+0.27±0.01**	1.3×10^{-2}–7.6×10^{-4}	4.5×10^{-4}–1.3×10^{-2}	0.9984
Sample 3 (intermediate quality)	**+0.49±0.01**	1.3×10^{-2}–7.6×10^{-4}	4.5×10^{-4}–1.3×10^{-2}	0.9988
Sample 4 (high quality)	**+0.81±0.01**	2.7×10^{-3}–7.1×10^{-5}	9.2×10^{-5}–2.8×10^{-3}	0.9990

crystal 4, which has the sharpest peak, can be found. Dots are the experimental data, while the continuous lines are the best fits to Eq. (7). The obtained critical exponent α together with the range of reduced temperature used in the fittings are shown in Table II. The sample with the poorest quality (sample 2), which exhibits a c_p shape similar to those previously published, has a positive critical exponent (α=0.27) not too far from the 3D-Ising behavior stated in Refs. 11 and 17. However, in samples 3 and 4, where the transition gets sharper (indicating a higher crystal quality), a higher α is obtained, which clearly deviates from the 3D-Ising model. In particular, the result for sample 4 (α=0.81) is exceptionally large and far away from any universality class. Moreover, following this trend, it is expected that crystals with a quality even higher than the best one used in this work could lead to a higher critical exponent. It is worth noting that high α values have already been reported, as is the case of $La_{0.7}Ca_{0.3}MnO_3$.[41] On the other hand, as no hysteresis has been found in any of the samples, there is no hint that the nature of the transition be other than second order, even if it is quite narrow and sharp.

IV. CONCLUSIONS

By using photopyroelectric calorimetry, we have simultaneously measured the thermal conductivity, the thermal diffusivity, and the specific heat of CoO and NiO in the vicinity of T_N. In the case of NiO, the critical exponent and amplitude ratio of c_p, D, and K agree with the predictions of the three-dimensional Heisenberg model for isotropic antiferromagnets. On the other hand, it has been found that the width and sharpness of the peak (dip) of specific heat (thermal diffusivity) in CoO at T_N strongly depend on crystal quality (defects, impurities, and magnetic twinning). Actually, the higher the crystal quality, the narrower and sharper the peak (dip) becomes. For the crystal with the best quality, an anomalously large critical exponent has been found (α=0.81). This result indicates that the critical behavior of CoO cannot be explained within any universality class.

ACKNOWLEDGMENTS

This work has been supported by the University of the Basque Country through research Grant No. EHU06/24.

*agustin.salazar@ehu.es

[1] W. L. Roth, Phys. Rev. **110**, 1333 (1958).
[2] S. A. Brazovskii and I. E. Dzyaloshinskii, Zh. Eksp. Teor. Fiz. **21**, 360 (1975) [JETP Lett. **21**, 164 (1975)].
[3] P. Bak, S. Krinsky, and D. Mukamel, Phys. Rev. Lett. **36**, 52 (1976).
[4] D. Mukamel and S. Krinsky, Phys. Rev. B **13**, 5078 (1976).
[5] D. Bloch, R. Maury, C. Vettier, and W. B. Yelon, Phys. Lett. **49A**, 354 (1974).
[6] D. Bloch, D. Hermann-Ronzaud, C. Vettier, W. B. Yelon, and R. Alben, Phys. Rev. Lett. **35**, 963 (1975).
[7] R. Boire and M. F. Collins, Can. J. Phys. **55**, 688 (1977).
[8] D. Bloch, C. Vettier, and P. Burlet, Phys. Lett. **75A**, 301 (1980).
[9] M. S. Jagadeesh and M. S. Seehra, Phys. Rev. B **23**, 1185 (1981).
[10] G. Srinivasan and M. S. Seehra, Phys. Rev. B **28**, 6542 (1983).
[11] M. B. Salamon, Phys. Rev. B **2**, 214 (1970).
[12] M. D. Rechtin, S. C. Moss, and B. L. Averbach, Phys. Rev. Lett. **24**, 1485 (1970).
[13] K. H. Germann, K. Maier, and E. Strauss, Phys. Status Solidi B **61**, 449 (1974).
[14] P. S. Silinsky and M. S. Seehra, Phys. Rev. B **24**, 419 (1981).
[15] C. Glorieux, J. Caerels, and J. Thoen, J. Phys. (Paris), Colloq. **4**, C7-267 (1994).
[16] J. Caerels, B. Maesen, and J. Thoen, Prog. Nat. Sci. **6**, S-254 (1996).
[17] F. J. Romero, J. Jiménez, and J. Del Cerro, J. Magn. Magn. Mater. **280**, 257 (2004).
[18] W. Jauch, M. Reehuis, H. J. Bleif, F. Kubanek, and P. Pattison, Phys. Rev. B **64**, 052102 (2001).
[19] K. H. Germann, K. Maier, and E. Strauss, Solid State Commun. **14**, 1309 (1974).
[20] C. F. Van Doorn and P. de V. Duplessis, Phys. Lett. **66A**, 141 (1978).
[21] I. Negovetić and J. Konstantinović, Solid State Commun. **13**, 249 (1973).
[22] M. B. Salamon, P. R. Garnier, B. Golding, and E. Buehler, J. Phys. Chem. Solids **35**, 851 (1974).

[23] M. Marinelli, F. Mercuri, U. Zammit, R. Pizzoferrato, F. Scudieri, and D. Dadarlat, Phys. Rev. B **49**, 9523 (1994).
[24] M. Marinelli, F. Mercuri, and D. P. Belanger, Phys. Rev. B **51**, 8897 (1995).
[25] C. Glorieux, J. Thoen, G. Bednarz, M. A. White, and D. J. W. Geldart, Phys. Rev. B **52**, 12770 (1995).
[26] M. Marinelli, F. Mercuri, S. Foglietta, and D. P. Belanger, Phys. Rev. B **54**, 4087 (1996).
[27] M. Marinelli, U. Zammit, F. Mercuri, and R. Pizzoferrato, J. Appl. Phys. **72**, 1096 (1992).
[28] M. Chirtoc, D. Dadarlat, D. Bicanic, J. S. Antoniow, and M. Egée, in *Progress in Photothermal and Photoacoustic Science and Technology*, edited by A. Mandelis and P. Hess (SPIE, Bellingham, Washington, 1997), Vol. 3; M. Chirtoc and G. Mihailescu, Phys. Rev. B **40**, 9606 (1989).
[29] S. Delenclos, M. Chirtoc, A. Hadj Sahraoui, C. Kolinsky, and J. M. Buisine, Rev. Sci. Instrum. **73**, 2773 (2002).
[30] A. Salazar, Rev. Sci. Instrum. **74**, 825 (2003).
[31] A. Salazar, M. Massot, A. Oleaga, A. Pawlak, and W. Schranz, Phys. Rev. B **75**, 224428 (2007).
[32] G. Ahlers, Rev. Mod. Phys. **52**, 489 (1980).
[33] A. Aharony and M. E. Fisher, Phys. Rev. B **27**, 4394 (1983).
[34] J. C. Le Guillou and J. Zinn-Justin, Phys. Rev. B **21**, 3976 (1980).
[35] V. Privman, P. C. Hohenberg, and A. Aharony, in *Phase Transitions and Critical Phenomena*, edited by C. Domb and J. L. Lebowitz (Academic, New York, 1991), Vol. 14.
[36] Most recent calculations of the critical exponent α for the 3D-Heisenberg universality class give $\alpha=-0.133$ and $\alpha=-0.121$ [A. Pelissetto and E. Vicari, Phys. Rep. **368**, 549 (2002); V. I. Yukalov and E. P. Yukalova, Eur. Phys. J. B **55**, 93 (2007)].
[37] A. Pawlak, Phys. Rev. B **68**, 094416 (2003).
[38] K. Kawasaki, Prog. Theor. Phys. **40**, 706 (1968).
[39] B. I. Halperin, P. C. Hohenberg, and E. Siggia, Phys. Rev. B **13**, 1299 (1976).
[40] P. C. Hohenberg and B. I. Halperin, Rev. Mod. Phys. **49**, 435 (1977).
[41] J. A. Souza, Yi-Kuo Yu, J. J. Neumeier, H. Terashita, and R. F. Jardim, Phys. Rev. Lett. **94**, 207209 (2005).